

A tale of two allotropes

Cite as: AIP Conference Proceedings **2150**, 020006 (2019); <https://doi.org/10.1063/1.5124578>
 Published Online: 03 September 2019

Francisco Pérez-Bernal, and Lorenzo Fortunato



View Online



Export Citation

ARTICLES YOU MAY BE INTERESTED IN

[Dynamical symmetries and beyond: Lessons and advances](#)

AIP Conference Proceedings **2150**, 020013 (2019); <https://doi.org/10.1063/1.5124585>

[Symmetries and regularities in nuclei: Order out of seeming chaos](#)

AIP Conference Proceedings **2150**, 020001 (2019); <https://doi.org/10.1063/1.5124573>

[Experimental evidence for dynamical supersymmetries as illustrated by \$^{195}\text{Pt}\$](#)

AIP Conference Proceedings **2150**, 020012 (2019); <https://doi.org/10.1063/1.5124584>

Lock-in Amplifiers up to 600 MHz

starting at

\$6,210



Zurich
Instruments

Watch the Video



A Tale of Two Allotropes

Francisco Pérez-Bernal^{1,2,a)} and Lorenzo Fortunato^{3,b)}

¹*Departamento de Ciencias Integradas y Centro de Estudios Avanzados en Física Matemáticas y Computación; Facultad de CC. Experimentales; Campus del Carmen; Universidad de Huelva, Huelva 21071 SPAIN.*

²*Also at Instituto Carlos I de Física Teórica y Computacional; Universidad de Granada, Granada 18071, SPAIN*

³*Dipartimento di Fisica e Astronomia “G. Galilei”, Università di Padova and I.N.F.N.- Sez. di Padova; v. Marzolo, 8, I-35131, Padova, ITALY*

^{a)}Corresponding author: curropb@uhu.es

^{b)}lorenzo.fortunato@pd.infn.it

Abstract. Making use of an algebraic model for the study of diatomic endofullerenes recently published [*Physical Review A* **94**, 032508 (2016)], we present a possible extension of this framework for the calculation of infrared intensities. We apply the model to the absorption infrared spectrum of $\text{H}_2@C_{60}$ at $T = 6$ K obtaining satisfactory preliminary results.

INTRODUCTION

Allotropy or allotropism refers to the existence of the same chemical element in two or more physical forms. A well-known example is carbon, that can be found as graphite, diamond, fullerenes, or graphene. In fact, one of the main characters of our tale of two allotropes is buckminsterfullerene, C_{60} . This molecule, considered by some as the most beautiful molecule, has icosahedral symmetry, the most complex point group symmetry. It is an empty sphere formed exclusively by carbon atoms. The discovery of fullerenes 1985 -also known as *buckyballs*- initiated a new branch of chemistry, with consequences in such diverse areas as astrochemistry, superconductivity and solid state physics. Soon after the discovery of fullerenes, the first *endofullerenes*, also called *endohedral fullerenes* were synthesized at the beginning of the 1990's trapping metal atoms into the carbon sphere [1]. These are supramolecular species, denoted as $A@C_N$ and formed by the confinement of a guest, A, into a buckyball. The guest is not bound to the fullerene carbon walls. On the contrary, the guest is incarcerated into the buckyball by a supramolecular (non-covalent) interaction. Some years later noble gases and then molecules were trapped into the buckyball [2]. Molecules trapped into fullerenes are considered the best example to date of a quantum rotor trapped into a spherical potential and the development of the so called *molecular surgery* techniques allowed the synthesis of endofullerenes in quantities large enough to apply different spectroscopic techniques and record the spectrum of the supramolecular species [3].

Endofullerenes are in the limelight due to their surprising quantum properties and because of many possible practical applications: in molecular electronics, in quantum information, or in radiodiagnostic by magnetic resonance are currently being explored. We focus our attention on the $\text{H}_2@C_{60}$ endofullerene [4, 5], with our second allotrope as guest: the hydrogen molecule. Hydrogen has two allotropes, *para* H_2 and *ortho* H_2 , that differ in their spin stereochemistry, the first has antiparallel proton spins configuration (singlet state) and the second parallel spins (triplet states). In order to comply with the Pauli selection rule, *para* and *ortho* H_2 only have even and odd molecular angular momentum, respectively. The coupling between spatial and spin properties make $\text{H}_2@C_{60}$ an excellent playground for the study of spin chemistry and spectroscopy. The small H_2 mass and the size of the space where the molecule is confined result in the quantization of the molecular center-of-mass translations and their coupling to the rovibrational degrees of freedom, having as an outcome particularly enticing quantum effects.

The coupling of these two sets of degrees of freedom hinders the problem of modeling the spectra of incarcerated diatomic species making necessary a 5D quantum model to encompass all the relevant degrees of freedom. The interest of an accurate description of supramolecular complexes as $\text{H}_2@C_{60}$ has produced very accurate phenomenological approaches to reproduce energies and intensities obtained in infrared [6, 7] and inelastic neutron scattering

[8, 9] experiments. In such phenomenological models $H_2@C_{60}$ states were labeled using the quantum numbers ν , J , n , L , and Λ , M_Λ . The number ν and J are the number of quanta of vibrational excitation in the molecule and its angular momentum with respect to the molecular center of mass. The labels n and L are the number of translational quanta and the angular momentum of the molecular center of mass with respect to the cage. Finally, Λ , M_Λ are the total angular momentum resulting from the coupling of J and L and its projection along an axis. With the aim of defining an algebraic model that could offer a computationally cheaper alternative to disentangle the interesting properties of diatomic endohedral species, we have recently presented an algebraic approach to the study of diatomic endofullerenes where, as an application, $H_2@C_{60}$ energies and state assignments were calculated from a fit to the available experimental data [10]. Our model reshapes the same physics of existing phenomenological approaches into an algebraic framework, providing an equivalent, but computationally simpler description that encompasses the main physical ingredients needed to achieve an accurate modeling of the quantum modes of a diatomic molecule confined in an isotropic three-dimensional cage. The algebraic Hamiltonian operator includes molecular rotational, vibrational, and center-of-mass modes, as well as the coupling of these two subsystems. The experimental term energies were obtained with two different techniques: infrared spectroscopy [7] and inelastic neutron scattering [11]. We aim to extend the results presented in [10] performing a fit to experimental infrared line intensities for $H_2@C_{60}$ at a temperature $T = 6$ K reported in [7, 12]. The initial ingredients are the energies and wave functions published in [10] and we define a new, enlarged, dynamical algebra and tentative infrared transition operators guided as in the previous work by symmetry considerations. By varying the three free parameters in such transition operator, we optimize the agreement with experimental infrared line intensities. The enlarged dynamical algebra sets a framework for accomplishing a fit that simultaneously encompass energies and intensities, and the present work is a first step towards this end.

As it would be clear for the reader in the next section, the algebraic model presented is strongly inspired by previous Franco Iachello works. Of course this will be completely clear for the reader in the second section, once he discovers that it is through the vibron model and its $u(4)$ dynamical algebra [13, 14] that we deal with molecular rotational and vibrational degrees of freedom. Nevertheless, taking into consideration the occasion on which this work is published, we think it is pertinent to include some lines about how Franco Iachello has and inspired us and influenced our professional careers.

In the case of LF, I came across Iachello's works during my PhD in Theoretical Nuclear Physics, mainly because of the new $E(5)$ solution of the Bohr hamiltonian. I soon realized I could find other solvable cases and this accomplishment brought me several praises. Little by little, I approached Lie algebras and group theory and reading Franco's papers was like opening a Pandora's box full of wonderfully crafted theories. His work is a constant source of inspiration and innovation, not only in nuclear, but also in molecular and particle physics. His profound dedication to this art is truly impressive.

In my case, FPB, I was introduced to Franco Iachello for the first time on June 22nd, 1993, when he was awarded the *Honoris Causa* PhD by the University of Sevilla. At that time I was an undergraduate student, close to the end of his major in Physics, that had already been strongly attracted by the beauty and elegance of group theory and algebraic methods in Physics. José Miguel Arias, and two visiting professors from UNAM, Renato Lemus and Alejandro Frank, introduced me to the symmetry way. On the ceremony, I was pleased to meet the famous Yale professor of which I had heard so much from the members of the Nuclear Physics group in Sevilla. Some years later, in 1997 and as a graduate student about to finish his PhD thesis, I visited Franco for the first time at Yale and spend some months there. It was a very fruitful period, when a research line on the calculation of Franck-Condon factors for polyatomic molecules was started [15]. This work was done in a close and very satisfactory collaboration with Pat Vaccaro and his graduate student Thomas Müller from the Chemistry Department (where Franco has a joined appointment) and others. Such a positive experience made me apply for a postdoc in Yale, where we proceeded with the Franck-Condon calculations applied to S_2O [16, 17, 18] and HCP [19], in the latter case introducing the 2D limit of the vibron model due to the geometric changes experienced by the molecule upon electronic excitation. This was only the beginning and the collaboration with Franco proceeded, with periodic stays in the Sloane Physics Laboratory to work on the description of the spectra and excitation of bending vibrations for non-rigid molecules in collaboration with Lea Santos [20, 21], QPTs and ESQPTs in the 2D limit of the vibron model [22, 23] or how to deal with coupled bending degrees of freedom in systems of interest, like acetylene [24, 25, 26]. My postdoc with Franco and every visit to him since, either in the USA or in Italy, had been unforgettable times that offered me the possibility of meeting many interesting people; many of them are nowadays great friends. But I would like to go beyond the bare scientific results and papers, notwithstanding the pleasure enjoyed in the collaborations that have produced this works. I want to stress the fact that Franco has been, from the very beginning, when he hosted me for the first time as a young student and visitor, a model both as a scholar and as a person. I consider a privilege to have had the wonderful opportunity of working

with somebody who owns a great generosity, an amazing physical insight, and a vast mathematical knowledge. On top of that I have enjoyed countless times his warm hospitality, his enlightening conversation and his deep knowledge of literature, poetry, art, history, or archaeology. Finally, I feel very glad and proud to count him as a friend and I hope that ours will be a lasting friendship with many interesting conversations to come.

ALGEBRAIC APPROACH TO ENDOFULLERENES

Dynamical Symmetry and Associated Basis

The dynamical symmetry proposed in [10] was defined in such a way that the rotations and vibrations of the diatomic molecule were described within the vibron model, introduced by Iachello in the 80's [13, 14, 27], associating a $u(4)$ Lie algebra to such molecular degrees of freedom. This algebra arises from the possible bilinear products of a creation and an annihilation operator based on two different bosons, a scalar s_p, s_p^\dagger ($\ell = 0$) and a vector p_μ, p_μ^\dagger ($\ell = 1, \mu = \pm 1, 0$) [28]. The fullerene cage was originally modeled as a spherical three dimensional well and making use of a $u(3)$ Lie algebra. This Lie algebra was built from a single vector boson operator q_μ, q_μ^\dagger ($\ell = 1, \mu = \pm 1, 0$) [29]. Thus, the algebraic model presented in [10] was based on the direct sum Lie algebra $u_p(4) \oplus u_q(3)$, where we used the sub-indexes p and q to distinguish the two different sets of degrees of freedom: molecular rotations and vibrations and the quantization of the molecular center of mass due to the interaction with the cage walls.

The consideration of infrared intensities and their associated selection rules requires an extension of this dynamical algebra, at least to simultaneously describe the wavefunctions involved in the transition and to enlarge the set of possible candidates for transition operator. This extension is performed *à la Iachello's*: including a new scalar boson, s_q, s_q^\dagger whose combination with the vector boson q_μ, q_μ^\dagger gives as a result a $u_q(4)$ Lie algebra for the description of the center of mass degrees of freedom [30].

The final dynamical algebra is $u_p(4) \oplus u_q(4)$ and the best dynamical symmetry to deal with endofullerenes studies is

$$\begin{array}{ccccccc} u_p(4) \oplus u_q(4) & \supset & so_p(4) \oplus u_q(3) & \supset & so_p(3) \oplus so_q(3) & \supset & so_{pq}(3) & \supset & so_{pq}(2) \\ N_p & & N_q & & \omega & & n_q & & J & & L & & \Lambda & & M_\Lambda \end{array}, \quad (1)$$

where we have closely followed the notation introduced in our previous work. The basis states can be labeled as $[[N_p N_q] \omega J; n_q L; \Lambda]$ or $[[N_p N_q] v J; n_q L; \Lambda]$ [31]. For the sake of brevity, we will remove the labels $[N_p N_q]$ that define the dynamical symmetry irrep and are common to all states. The set of quantum numbers $(v J N_q L \Lambda)$ corresponds to the state labels used so far in theoretical investigations, enhancing the connection with Refs. [6, 7, 8, 11, 32, 5].

The basis quantum numbers follow well-known branching rules [27, 29]

$$\begin{aligned} \omega &= N_p, N_p - 2, \dots, 1 \text{ or } 0, \\ n_q &= N_q, N_q - 1, \dots, 0, \\ J &= 0, 1, \dots, \omega, \\ L &= N_q, N_q - 2, \dots, 1 \text{ or } 0, \\ \Lambda &= |J - L|, |J - L| + 1, \dots, J + L. \\ M_\Lambda &= -\Lambda, -\Lambda + 1, \dots, \Lambda - 1, \Lambda. \end{aligned} \quad (2)$$

Model Hamiltonian

The total Hamiltonian can be written as

$$\hat{H}_{endo} = \hat{H}_{u_p(4)} + \hat{H}_{u_q(4)} + \hat{H}_{Coupl}, \quad (3)$$

where the first and second terms are the vibron model Hamiltonian for rotations and vibrations of the diatomic guest [33] and the Hamiltonian modeling the motion of the molecular center-of-mass inside a three-dimensional spherically-symmetric confining potential. The third term includes the couplings between the center of mass and rotational and vibrational degrees of freedom. As we proceed to show, the goodness of the basis defined in (1) is clear when we realize that, using the same Hamiltonian operators than in Ref. [10], the $\hat{H}_{u_p(4)}$ and $\hat{H}_{u_q(4)}$ operators are diagonal and \hat{H}_{Coupl} is the only non-diagonal contribution.

The $u(4)$ vibron model Hamiltonian contains Casimir operators of the $so(4)$ dynamical symmetry [33, 27], the first two terms are standard two-body operators, and the other two are higher-order contributions, the third is a centrifugal correction and the fourth a rotation-vibration coupling.

$$\hat{H}_{u_p(4)} = E_0 + \beta \hat{C}_2[so_p(4)] + \gamma \hat{C}_2[so_p(3)] + \gamma_2 \hat{C}_2[so_p(3)]^2 + \kappa \hat{C}_2[so_p(4)]\hat{C}_2[so_p(3)]. \quad (4)$$

The Casimir operators in Equation (4) are diagonal in the chosen basis (1)

$$\begin{aligned} \langle \alpha | \hat{C}_2[so_p(4)] | \alpha \rangle &= \omega(\omega + 2), \\ \langle \alpha | \hat{C}_2[so_p(3)] | \alpha \rangle &= J(J + 1), \\ \langle \alpha | \hat{C}_2[so_p(4)]\hat{C}_2[so_p(3)] | \alpha \rangle &= \omega(\omega + 2)J(J + 1), \end{aligned} \quad (5)$$

where $|\alpha\rangle = |\omega J; n_q L; \Lambda\rangle$.

The energy formula obtained for $\hat{H}_{u_p(4)}$ is

$$\begin{aligned} E_{u_p(4)} &= E_0 + \beta \omega(\omega + 2) + \gamma J(J + 1) \\ &+ \gamma_2 \left[J(J + 1) \right]^2 + \kappa \left[\omega(\omega + 2)J(J + 1) \right], \end{aligned} \quad (6)$$

where $\omega = N_p, N_p - 2, \dots, 1$ or 0 or, alternatively, $v = 0, 1, \dots, \frac{1}{2}(N_p - 1)$ or $\frac{1}{2}N_p$ and $J = 0, 1, \dots, \omega$.

The center-of-mass degrees of freedom Hamiltonian, within the $u_q(4)$ dynamical symmetry, is kept the same than in the precious work

$$\hat{H}_{u_q(4)} = a \hat{C}_1[u_q(3)] + b \hat{C}_2[u_q(3)] + c \hat{C}_2[so_q(3)], \quad (7)$$

where the first term is the number of q bosons, the second term is an anharmonic correction, and the third term is the H_2 center-of-mass centrifugal energy.

Again the Casimir operators are diagonal in the chosen basis (1)

$$\begin{aligned} \langle \alpha | \hat{C}_1[u_q(3)] | \alpha \rangle &= n_q, \\ \langle \alpha | \hat{C}_2[u_q(3)] | \alpha \rangle &= n_q^2, \\ \langle \alpha | \hat{C}_2[so_q(3)] | \alpha \rangle &= L(L + 1), \end{aligned} \quad (8)$$

where $|\alpha\rangle$ is again $|\omega J; n_q L; \Lambda\rangle$. The resulting energy formula is

$$E_{u_q(4)} = a n_q + b n_q^2 + c L(L + 1), \quad (9)$$

where n_q is the eigenvalue of the number of quanta operator and L is the orbital angular momentum of the whole confined particle (*viz.* the center of mass of the H_2 molecule) inside the fullerene cage.

In regard with the coupling between the center of mass and rovibrational degrees of freedom, the guest diatomic molecule and the cage interact through a number of different physical mechanisms, and we have found that the relevant terms imply quadropole-quadropole couplings [10].

The algebraic scheme provides the quadropole operators of $u_p(4)$ and $u_q(4)$, namely $\hat{Q}_t = [t^\dagger \times \tilde{t}]^{(2)}$, where $t = p, q$. A scalar coupling can be built from these two operators as $[\hat{Q}_p^{(2)} \times \hat{Q}_q^{(2)}]^{(0)}$. This operator lifts the degeneracy of $\Lambda \neq 0$ multiplets and gives as a result the unusual level ordering recorded in experiments and is the basis for the coupling terms in the Hamiltonian (3). In addition, with the aim of optimizing the agreement with experimental data, higher order terms were considered in the coupling Hamiltonian:

$$\hat{H}_{Coupl} = \vartheta_{pq} [\hat{Q}_p^{(2)} \times \hat{Q}_q^{(2)}]^{(0)} + \vartheta_{pqw} \left[\hat{C}_2[so_p(4)] [\hat{Q}_p^{(2)} \times \hat{Q}_q^{(2)}]^{(0)} + [\hat{Q}_p^{(2)} \times \hat{Q}_q^{(2)}]^{(0)} \hat{C}_2[so_p(4)] \right] + v_{pq} \hat{C}_1[u_q(3)] \hat{C}_2[so_p(4)]. \quad (10)$$

For the sake of self-consistency, we provide the matrix elements of the scalar coupling $[\hat{Q}_p^{(2)} \times \hat{Q}_q^{(2)}]^{(0)}$ [34]

$$\langle \omega J; n_q L; \Lambda | [\hat{Q}_p^{(2)} \times \hat{Q}_q^{(2)}]^{(0)} | \omega' J'; n'_q L'; \Lambda' \rangle = (-1)^{L+\Lambda+J'} \sqrt{5} \begin{Bmatrix} J & L & \Lambda \\ L' & J' & 2 \end{Bmatrix} \langle n_q L | \hat{Q}_q | n'_q L' \rangle \langle \omega J | \hat{Q}_p | \omega' J' \rangle \delta_{\Lambda, \Lambda'}. \quad (11)$$

Once we separate the molecular and cage degrees of freedom, the reduced matrix elements of the molecular (\hat{Q}_p) and center-of-mass (\hat{Q}_q) quadrupole degrees of freedom are [27]

$$\begin{aligned}
\langle n_q L || \hat{Q}_q || n_q L \rangle &= (2n_q + 3) \sqrt{\frac{L(L+1)(2L+1)}{6(2L-1)(2L+3)}}, \\
\langle n_q L + 2 || \hat{Q}_q || n_q L \rangle &= \sqrt{\frac{(n_q - L)(n_q + L + 3)(L+1)(L+2)}{(2L+3)}}, \\
\langle \omega 0 || \hat{Q}_p || \omega 0 \rangle &= 0, \\
\langle \omega J || \hat{Q}_p || \omega J \rangle &= (N_p + 2) \left(1 + \frac{J(J+1)}{\omega(\omega+2)} \right) \sqrt{\frac{J(J+1)(2J+1)}{6(2J-1)(2J+3)}}, \\
\langle \omega J + 2 || \hat{Q}_p || \omega J \rangle &= (N_p + 2) \sqrt{\frac{(\omega - J - 1)_2 (\omega + J + 2)_2 (J+1)(J+2)}{4\omega^2 (\omega + 2)^2 (2J+3)}}, \\
\langle \omega + 2J - 2 || \hat{Q}_p || \omega J \rangle &= \sqrt{\frac{(N_p - \omega)(N_p + \omega + 4)(\omega - J + 1)_4 J(J-1)}{16(\omega + 1)_3 (\omega + 2)(2J-1)}}, \\
\langle \omega + 2J || \hat{Q}_p || \omega J \rangle &= \sqrt{\frac{(N_p - \omega)(N_p + \omega + 4)(\omega - J + 1)_2 (\omega + J + 2)_2 J(J+1)(2J+1)}{24(\omega + 1)_3 (\omega + 2)(2J-1)(2J+3)}}, \\
\langle \omega + 2J + 2 || \hat{Q}_p || \omega J \rangle &= \sqrt{\frac{(N_p - \omega)(N_p + \omega + 4)(\omega + J + 2)_4 (J+1)(J+2)}{16(\omega + 1)_3 (\omega + 2)(2J+3)}},
\end{aligned}$$

where we use the Pochhammer symbol $(a)_b = a(a+1)\cdots(a+b-1)$. Note that the enlargement of the original dynamical symmetry from $u_p(4) \oplus u_q(3)$ to $u_p(4) \oplus u_q(4)$ does not affect these matrix element due to the fact that the center-of-mass quadrupole (\hat{Q}_q) belongs to the $u_q(3) \in u_q(4)$.

The matrix elements for the other two operators in the coupling Hamiltonian (10), $[\hat{C}_2[so_p(4)][\hat{Q}_p^{(2)} \times \hat{Q}_q^{(2)}]^{(0)} + [\hat{Q}_p^{(2)} \times \hat{Q}_q^{(2)}]^{(0)} \hat{C}_2[so_p(4)]$ and $\hat{C}_1[u_q(3)]\hat{C}_2[so_p(4)]$, are trivially computed using Equation (5), (8), and (11).

The model Hamiltonian has a total of 10 free parameters whose values, as explained in [10], were fixed to achieve the better possible agreement with the available set of experimental data, obtaining a satisfactory agreement with the experiment. We performed two fits, denoted as fit F_0 and F_1 . The first one includes 7 parameters, leaving aside γ_2 , ϑ_{pqw} , and ν_{pq} , while the second one includes all the parameters. It is especially interesting how the characteristic level splitting due to the interaction between translational and rovibrational degrees of freedom, shown in Figure 1 can be reproduced with the inclusion of the quadrupole-quadrupole coupling interaction

INFRARED LINE INTENSITY AND TRANSITION OPERATOR

We follow closely Ref. [7] for the calculation of the infrared absorption line areas. In principle, the H_2 molecule dipole moment is zero, as happens with all homonuclear diatomic molecular species, however the interaction between the molecule and the cage in the translational motion results in an induced dipole moment.

From Ref. [7] the infrared absorption line area between states $|i\rangle$ and $|f\rangle$, that is the experimentally reported quantity, is denoted as $S(\omega_{if})$ and is expressed as follows

$$S(\omega_{if}) = \frac{N}{V} \frac{\pi 10^{-2}}{3\eta\hbar c \epsilon_0} p_i \omega_{if} |\langle f || d^{(1)} || i \rangle|, \quad (12)$$

where all units are SI but ω in cm^{-1} and $S(\omega_{if})$ in cm^{-2} . The different quantities involved are $\frac{N}{V} = 1.48 \times 10^{27} \text{ m}^{-3}$, the number density of molecules in solid C_{60} ; ϵ_0 , the permittivity of vacuum; $\eta = 2$, the C_{60} index of refraction; p_i , the probability that the initial state is populated; $\omega_{if} = (E_f - E_i)/(2\pi\hbar c)$; and $d^{(1)}$ is the endofullerene H_2 induced dipole moment.

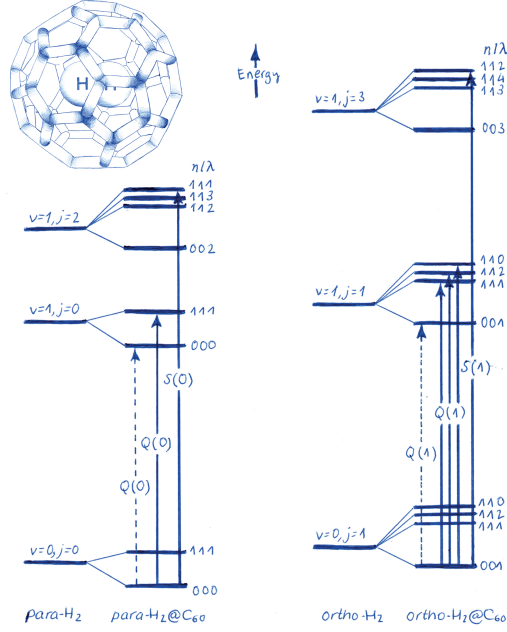


FIGURE 1. Lowest energy levels and the corresponding IR spectroscopy transitions for *para* (left) and *ortho* (right) $\text{H}_2@C_{60}$ at low temperatures. Dashed lines stand for forbidden transitions. The incarceration of H_2 into the buckyball originates the splittings of the unperturbed molecule rovibrational energy levels into translational sublevels labeled by quantum numbers n , l , and λ , as discussed in the text. For the sake of clarity, in the ground vibrational $v = 0$ state only the $j = 1$ energy level is shown.

The probability that the $|i\rangle$ state is populated can be computed as [7]

$$p_i = \frac{n_k(2\Lambda_i + 1) \exp\left(-\frac{E_i}{k_B T}\right)}{\sum_j (2\Lambda_j + 1) \exp\left(-\frac{E_j}{k_B T}\right)}, \quad (13)$$

where the sum in j runs over all *para* or *ortho* states, E_i is the initial state excitation energy from the $n_q = v = 0$ state, and n_k with $k = o, p$ the fractional *ortho* and *para* populations.

From the wave functions and energy spectra obtained in the fit reported in [10], all quantities in Equation (12) can be computed apart from the induced dipole moment reduced matrix elements $\langle f || d^{(1)} || i \rangle$. In the present work we suggest a possible algebraic realization of such infrared transition operator, denoted as $\hat{d}^{(1)}$. The defined induced dipole moment complies with the selection rules for infrared transitions: $\Delta n_q = \pm 1$, $\Delta L = \pm 1$, $\Delta J = 0, \pm 2$, and $\Delta \Lambda = 0, \pm 1$ [7, 32] for endofullerenes and depends on two operators that couple molecular rovibrational and translational degrees of freedom

$$\hat{d}^{(1)} = \delta_0^{(1)} [n_p \times \hat{D}'_q]^{(1)} + \delta_1^{(1)} [\hat{Q}^{(2)} \times \hat{D}'_q]^{(1)}, \quad (14)$$

where $\delta_i^{(1)}$ with $i = 0, 1$ are free parameters to optimize the agreement with experimental absorption line areas.

The reduced matrix elements of the induced dipole moment operator (14) in the basis (1) were not reported in [10] because the \hat{D}'_q algebra elements were not originally considered. They stem from the extension of $u_q(3)$ to $u_q(4)$. The reduced matrix elements of the two operators in (14) are

$$\begin{aligned} \langle \omega J; n_q L; \Lambda || [\hat{n}_p \times \hat{D}'_q]^{(1)} || \omega' J'; n'_q L'; \Lambda' \rangle &= \sqrt{3(2\Lambda + 1)(2\Lambda' + 1)} \begin{Bmatrix} J & L & \Lambda \\ J' & L' & \Lambda' \\ 0 & 1 & 1 \end{Bmatrix} \\ &\times \langle n_q L || \hat{D}'_q || n'_q L' \rangle \langle \omega J || \hat{n}_p || \omega' J' \rangle, \end{aligned} \quad (15)$$

$$\langle \omega J; n_q L; \Lambda \| [\hat{Q}_p^{(2)} \times \hat{D}'_q]^{(1)} \| \omega' J'; n'_q L'; \Lambda' \rangle = \sqrt{3(2\Lambda + 1)(2\Lambda' + 1)} \begin{Bmatrix} J & L & \Lambda \\ J' & L' & \Lambda' \\ 2 & 1 & 1 \end{Bmatrix} \times \langle n_q L \| \hat{D}'_q \| n'_q L' \rangle \langle \omega J \| \hat{Q}_p \| \omega' J' \rangle. \quad (16)$$

The relevant reduced matrix elements of the operator \hat{n}_p in the $so_p(4)$ basis are [27]

$$\langle \omega J \| \hat{n}_p \| \omega J \rangle = \frac{N_p - 1}{2} \sqrt{2J + 1} + \frac{(N_p + 2)J(J + 1)(2J + 1)}{2w(w + 2)}, \quad (17)$$

$$\langle \omega + 2J \| \hat{n}_p \| \omega J \rangle = \sqrt{\frac{(2J + 1)(N_p - w)(N_p + w + 4)(\omega - J + 1)_2(w + J + 2)_2}{16(w + 2)(w + 1)_3}}, \quad (18)$$

while in the case of the reduced matrix elements of \hat{D}'_q in the $u_q(3)$ basis, the required elements are [27]

$$\langle n_q + 1L - 1 \| \hat{D}'_q \| n_q L \rangle = \sqrt{(N_q - n_q)(n_q - L + 2)L}, \quad (19)$$

$$\langle n_q + 1L + 1 \| \hat{D}'_q \| n_q L \rangle = \sqrt{(N_q - n_q)(n_q + L + 3)(L + 1)}. \quad (20)$$

FIT RESULTS TO INFRARED LINE INTENSITIES

As a preliminary test of the algebraic dipole transition operator (14) we perform a non-linear least-squares fit to the experimental IR absorption line areas reported in [7] and optimize the parameters $\delta_i^{(1)}$ with $i = 1, 2$ and $n_{op} = n_o/n_p$, the ortho to para ratio [35]. We would like to emphasize that the wavefunctions and state term values used are the ones obtained in the fit labeled as fit F_1 in [10], obtained without taking into consideration the experimental intensities and with a dynamical algebra $u_p(4) \oplus u_q(3)$. The optimized parameter values are

TABLE 1. Optimized values of the algebraic dipole moment transition operator parameters $\delta_i^{(1)}$, $i = 0, 1$, to reproduce the IR spectrum of $H_2@C_{60}$ at 6 K, the *ortho* to *para* ratio n_{op} , the values of the N_p and N_q parameters determining the irrep of the dynamical algebra used in the calculations, and the final reported root mean square, *rms*, of the fit. We report the optimized values obtained with wavefunctions from the fits F_0 and F_1 published in [10].

Parameter Units	$\delta_0^{(1)}$ cm ⁻²	$\delta_1^{(1)}$ cm ⁻²	n_{op}	N_p	N_q	<i>rms</i> cm ⁻²
Fit F_0	0.0097(5)	0.0138(16)	0.95(12)	34	20	1.236
Fit F_1	0.0062(6)	0.0118(24)	1.5(4)	34	20	1.235

The results obtained for parameter in Table 1 are depicted in Fig. 2. The *synthetic spectrum* is computed from the available experimental data for the IR spectrum of $H_2@C_{60}$ at 6 K using Gaussian lineshapes with $FWHM = 1 \text{ cm}^{-1}$ [7, 12]; it is depicted with blue crosses in Fig. 2. The results obtained with the optimized parameters reported in Table 1 are drawn with full orange and red lines. Orange (red) lines correspond to the $H_2@C_{60}$ wave functions from fits F_0 (F_1) in [10]. As expected from the quality of the energy fit F_1 in [10] the line positions are better reproduced in this case, nevertheless the agreement between calculated and experimental IR absorption line areas is basically the same in both cases, as can be deduced from the similar values obtained for the *rms* in both cases (last column in Table 1). Thus the results of this preliminary calculation indicate that the basic physical ingredients needed to reproduce the spectrum are already present in the wave functions obtained from a basic fit F_0 . As we detail in the next section, we plan to improve this preliminary result in the near future either performing calculations with a modified induced dipole moment algebraic realization, or taking advantage of the extension of the model to a $u_p(4) \oplus u_q(4)$ dynamical algebra and performing a simultaneous fit to term energies and line intensities.

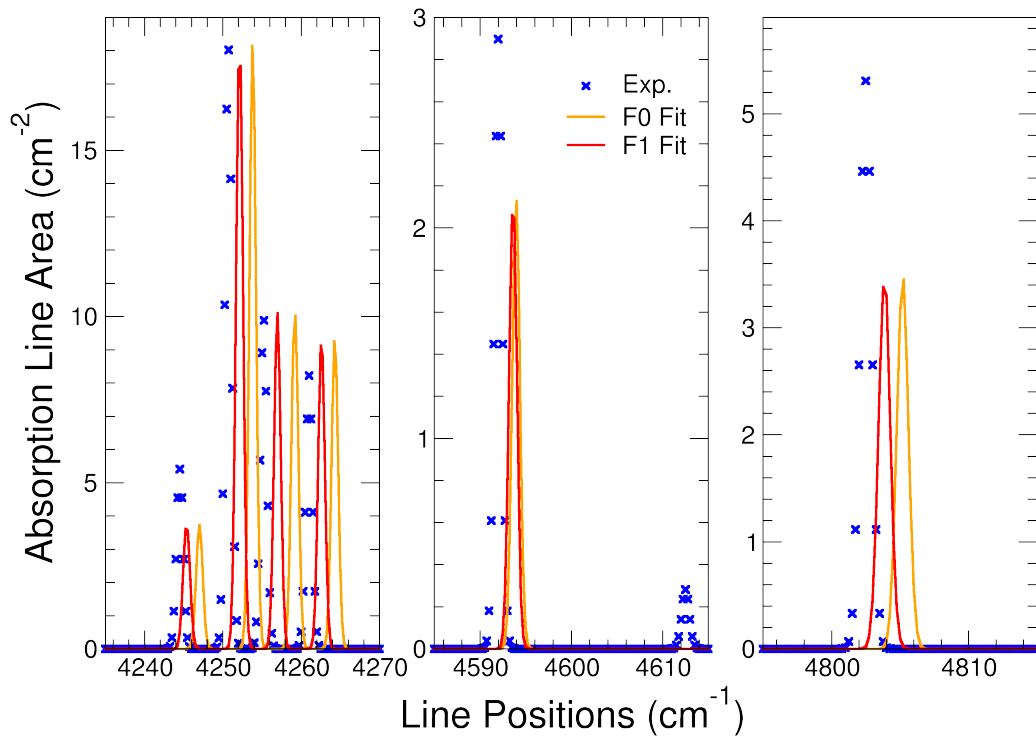


FIGURE 2. IR absorption line areas for $\text{H}_2@C_{60}$ at 6 K as a function of transition wavelength. The synthetic spectrum computed from the experimental information [7, 12] is depicted using blue crosses. The absorption spectrum computed from the wavefunctions and energies obtained in fit F_0 (F_1), Equation (12), induced dipole moment algebraic realization (14), and parameters in Table 1 [10] is depicted with full orange (red) lines.

CONCLUDING REMARKS

In the present work we have presented the theoretical formalism to enlarge the dynamical algebra of the algebraic approach to diatomic endohedral species presented in [10] from the original $u_p(4) \oplus u_q(3)$ to a $u_p(4) \oplus u_q(4)$ dynamical algebra. As an application we have proposed an algebraic form for the $\text{H}_2@C_{60}$ induced dipole moment that depends on two free parameters and performed a preliminary calculation of infrared absorption intensities for $\text{H}_2@C_{60}$ at a temperature $T = 6$ K [7] from the wave functions of fits F_0 and F_1 reported in [10]. The final results obtained, shown in Figure 2, have a qualitatively acceptable agreement with the reported experimental synthetic spectrum, although there is still ample room for improvement as the agreement with the experimental data shows a certain amount of redshift and differences between computed and experimental infrared absorption areas. As we mentioned in the previous section, comparing the *rms* values reported in Table 1, we find quite remarkable that the intensities computed using the wave functions from fit F_0 have a similar agreement with the experimental infrared absorption areas than the intensities computed making use of the wave functions from fit F_1 that has three extra operators in the Hamiltonian. The line positions improve in the second case, as expected from the improved energy fit, but the optimized intensities have the same agreement with the experimental data.

We plan to improve this initial results by working in different aspects of the model. The first step that we will take to improve the reported results is to extend the results to the 200 K data reported in [7] and perform a simultaneous fit of energies and intensities. This fit could be done in two ways. On the one hand we can fit energies and line intensities

in the same way that we have done in [10] and in the present work, though with a fit that combines the information on energies and line intensities. In our experience the fit of intensities is a stringent test on the quality of the fit and in several occasions comparable fits considering only the energy spectrum have utterly different results when intensities are computed [19, 36]. Another possibility is to follow a procedure similar to the one described in [7], and fitting the model outcome to a synthetic spectrum.

The simultaneous fit of energies and intensities will be combined with the search of improved algebraic realizations of the induced dipole moment operator $d^{(1)}$. In fact the correct algebraic realization of $d^{(1)}$ may help explaining why the induced dipole moment is suppressed for transitions in the ground vibrational state, solving the conundrum of the non observation of $\Delta n_q = \pm 1$ with $\Delta v = 0$. Such transitions should be accessible experimentally if one considers the modeling results of the present model and of the model of Ge *et al.* [7].

Another possibility open for improvement of the reported results is the exploration of the possibilities opened up with the enlargement of the system dynamical symmetry to $u_p(4) \oplus u_q(4)$. The new dynamical algebra allows for the inclusion of couplings between states with different n_q . Considering our previous remark, this could improve the agreement with experimental line intensities though the resulting energies may not be greatly affected.

We consider that the present model is a computationally efficient approach to the structure of diatomic molecular species confined into fullerenes. We have already shown the advantages offered by a symmetry-guided algebraic approach to these fascinating quantum systems, obtaining a good agreement to the $\text{H}_2@C_{60}$ experimental spectrum making use of Hamiltonian (3), identifying the key coupling as the quadrupole-quadrupole interaction between rovibrational and translational degrees of freedom. We expect that once we find an appropriate algebraic realization of the induced dipole moment equivalent results will be obtained for the intensities, improving our comprehension of endohedral compounds with a simple yet powerful model that follows the trail so brilliantly marked by Franco Iachello and his many contributions in the description of very different physical systems with the common denominator of an acute quest for beauty and elegance through the use of symmetry for the description of natural phenomena.

ACKNOWLEDGMENTS

FPB thanks the Spanish MINECO grant FIS2014-53448-C2-2-P and the support obtained from the Centro de Estudios Avanzados en Física Matemáticas y Computación (CEAFMC) of the University of Huelva.

REFERENCES

- [1] Y. Chai *et al.*, *J. Phys. Chem.* **95**, 7564–7568 (1991).
- [2] M. Saunders *et al.*, *Science* **271**, 1693–1697 (1996).
- [3] K. Komatsu, M. Murata, and Y. Murata, *Science* **307**, 238–240 (2005).
- [4] N. J. Turro *et al.*, *Acc. Chem. Res.* **43**, 335–345 (2010).
- [5] S. Mamone *et al.*, *Coord. Chem. Rev.* **255**, 938 – 948 (2011).
- [6] M. Xu *et al.*, *J. Chem. Phys.* **128**, p. 011101 (2008).
- [7] M. Ge *et al.*, *J. Chem. Phys.* **134**, p. 054507 (2011).
- [8] M. Xu and Z. Bačić, *Phys. Rev. B* **84**, p. 195445 (2011).
- [9] M. Xu, S. Ye, and Z. Bačić, *J. Phys. Chem. Lett.* **6**, 3721–3725 (2015).
- [10] L. Fortunato and F. Pérez-Bernal, *Phys. Rev. A* **94**, p. 032508 (2016).
- [11] A. J. Horsewill *et al.*, *Phys. Rev. B* **85**, p. 205440 (2012).
- [12] T. Room, Private Communication (2017).
- [13] F. Iachello, *Chem. Phys. Lett.* **78**, 581 – 585 (1981).
- [14] F. Iachello and R. D. Levine, *Algebraic Theory of Molecules*, Topics in physical chemistry series (Oxford University Press, USA, 1994).
- [15] T. Müller *et al.*, *Chem. Phys. Lett.* **292**, 243 – 253 (1998).
- [16] T. Müller, P. H. Vaccaro, F. Pérez-Bernal, and F. Iachello, *J. Chem. Phys.* **111**, 5038–5055 (1999).
- [17] T. Müller, P. Vaccaro, F. Pérez-Bernal, and F. Iachello, *Chem. Phys. Lett.* **329**, 271 – 282 (2000).
- [18] F. Iachello, F. Pérez-Bernal, T. Müller, and P. H. Vaccaro, *J. Chem. Phys.* **112**, 6507–6510 (2000).
- [19] H. Ishikawa *et al.*, *Chem. Phys. Lett.* **365**, 57 – 68 (2002).
- [20] F. Iachello, F. Pérez-Bernal, and P. Vaccaro, *Chem. Phys. Lett.* **375**, 309 – 320 (2003).
- [21] F. Pérez-Bernal, L. Santos, P. Vaccaro, and F. Iachello, *Chem. Phys. Lett.* **414**, 398 – 404 (2005).
- [22] F. Pérez-Bernal and F. Iachello, *Phys. Rev. A* **77**, p. 032115Mar (2008).

- [23] D. Larese, F. Pérez-Bernal, and F. Iachello, *J. Mol. Struct.* **1051**, 310 – 327 (2013).
- [24] F. Iachello and F. Pérez-bernal, *Mol. Phys.* **106**, 223–231 (2008).
- [25] F. Iachello and F. Pérez-Bernal, *J. Phys. Chem. A* **113**, 13273–13286 (2009).
- [26] D. Larese, M. A. Caprio, F. Pérez-Bernal, and F. Iachello, *J. Chem. Phys.* **140**, p. 014304 (2014).
- [27] A. Frank and P. van Isacker, *Algebraic Methods in Molecular and Nuclear Structure Physics* (John Wiley and Sons, New York, 1994).
- [28] F. Iachello, *Chem. Phys. Lett.* **78**, 581 – 585 (1981).
- [29] F. Iachello, *Lie Algebras and Applications*, Lecture Notes in Physics, Vol. 891 (Springer, 2nd Edition, Berlin, 2015).
- [30] F. Iachello, in *Contemporary Mathematics*, Vol. 160 (American Mathematical Society, Providence, RI, 1994), pp. 151–171.
- [31] Note1, The ω label is related to the diatomic vibrational quantum number ν through $\nu = \frac{1}{2}(N_p - \omega)$.
- [32] S. Mamone *et al.*, *J. Chem. Phys.* **130**, p. 081103 (2009).
- [33] F. Iachello and R. D. Levine, *Algebraic Theory of Molecules*, Topics in physical chemistry series (Oxford University Press, USA, 1994).
- [34] A. Shalit and I. Talmi, *Nuclear Shell Theory*, Pure and applied physics (Academic Press, 1963).
- [35] Note2, We have extended the original Python code to compute intensities as well as energies and wave functions within the algebraic model. The parameter optimization was performed with LMFIT a non-linear least-squares minimization and curve-fitting package for Python.
- [36] R. Lemus, M. Sánchez-Castellanos, F. Pérez-Bernal, J. M. Fernández, and M. Carvajal, *J. Chem. Phys.* **141**, p. 054306 (2014).
- [37] F. Iachello and A. Arima, *The Interacting Boson Model* (Cambridge University Press, Cambridge, 1987).